Received January 18, 2018; | Revised ; | Accepted

DOI: xxx/xxxx

RESEARCH ARTICLE

A general method to stabilize unstable periodic orbits for switched dynamical systems with a periodically moving threshold

Yuu Miino[1] | Daisuke Ito[2] | Hiroyuki Asahara[3] | Takuji Kousaka*[4] | Tetsushi Ueta[5]

[1]Graduate school of Advanced Technology and Science, Tokushima University, 2–1 Minami-Josanjima, Tokushima, Japan
[2]Department of Electrical, Electronic and Computer Engineering, Gifu University, 1-1 Yanagido Gifu, Japan
[3]Department of Electrical and Electronic Engineering, Okayama University of Science, 1-1 Ridai-cho, Kita-ku, Okayama, Japan
[4]Department of Mechanical and Energy Systems Engineering, Oita University, 700 Dannoharu, Oita, Japan
[5]Center for Administration of Information Technology, Tokushima University, 2–1 Minami-Josanjima, Tokushima, Japan

Correspondence
*Takuji Kousaka, Department of Mechanical and Energy Systems Engineering, Oita University, 700 Dannoharu, Oita, Japan,
Email: takuji@oita-u.ac.jp

Abstract

In the previous study, a method to control chaos for switched dynamical systems with constant threshold value has been proposed. In this paper, we extend this method to the systems including a periodically moving threshold. The main control scheme is based on the pole placement, then a small control perturbation added to the moving threshold value can stabilize an unstable periodic orbit embedded within a chaotic attractor. For an arbitrary periodic function of the threshold movement, we mathematically derive the variational equations, the state feedback parameters, and a control gain by composing a suitable Poincaré map. As examples, we illustrate control implementations for systems with thresholds whose movement waveforms are sinusoidal and sawtooth-shape, and unstable one and two periodic orbits in each circuit are stabilized in numerical and circuit experiments. In these experiments, we confirm enough convergence of the control input.

KEYWORDS:
controlling chaos; switched dynamical system; numerical simulation; circuit implementation

1 | INTRODUCTION

Chaos is the disorderly states appeared in deterministic dynamical systems modeled in various scientific fields such as chemistry, ecology, medicine, economy and so on. Following three properties are the essential characteristics of chaos: sensitivity to initial conditions, topological mixing, dense unstable periodic orbits (UPOs)[1]. In these days, chaos has been focused on with the interests of practical applications. In the field of communications technology, the methods to generate a secret key or a quasirandom number using chaos is developed[2,3]. In biology, Aihara has proposed the model of a neuron with chaotic dynamics[4]. The model composes the chaotic neural network used for the optimization of some objective functions. In environmental engineering, Huang has developed chaos prediction using the Lyapunov exponent and its application in water quality forecast[5]. On the other hand, from a long time ago, many researchers in engineering have studied how to avoid chaos since such random, noisy, unpredictable responses are treated as repulsive behavior. As the method to solve this problem, stabilization of the UPOs embedded in chaos by applying a small control input has been well studied from the theoretical and experimental standpoints. The method is reasonable because the control input finally vanishes. For example, Ott et al. proposed a method targeting discrete-time dynamical systems[6], and Pyragas proposed the delayed feedback control dealing with continuous-time dynamical systems[7]. Other than them, there are various controlling methods: impulsive control[8], sliding mode control[9], linear feedback control[10] and so on[11,12,13,14].

We discussed a switched dynamical system described by an evolution equation including conditions depending on the states or the past time [15]. In these systems, there exist various bifurcation phenomena or chaos as the parameters vary. Banerjee has well studied these systems and has indicated that there exist some conspicuous phenomena in the systems [16]. On the other hand, Kousaka has analyzed the stability of the periodic solutions of the switched dynamical systems and has obtained bifurcation sets in the parameter plane [17]. In power electronics, power converters, such as a DC-DC converter, belong to these systems, and some researchers have presented chaos under the influence of its switching [16,18]. Since these circuits have been well used in practical industrial purpose, developing the method to control chaos in the systems is important and, indeed, several controlling methods have been experimentally studied [19,20,21,22]. In these days, Ito [23] has developed a new method to control chaos in switched dynamical systems with perturbing the threshold value. However, this study assumed that the reference threshold value is fixed; and the method simply perturbs the threshold value slightly by following linear control theory. In practice, the threshold might take various periodical waveforms, e.g., sine waves, sawtooth waves. A bouncing-ball system discussed in mechanics is a example including the moving threshold [24]. The model simulates the movement of a particle over a periodically moving table. The sinusoidal pulse width modulation [25] also includes the sinusoidal reference voltage. This scheme realizes an inverter, which produces an AC output from a DC input.

In this study, we develop a general method to control the chaos in the switched dynamical systems based on the method in Ref. [23]. We construct a method that can deal with any kind of the threshold value with periodic movement. Firstly, assuming that the target system is an n-dimensional switched dynamical system, we mathematically derive the variational equations, the state feedback parameters, and a control gain with a suitable Poincaré map. From the variation equation of the fixed point, we derive a control vector to stabilize the unstable periodic point. The main control scheme is based on the pole placement [26] and a small control perturbation added on the moving threshold value stabilizes an unstable periodic orbit embedded within a chaotic attractor. Next, we implement the method with the mathematical models including two typical thresholds: a sine wave threshold and a sawtooth wave threshold. We concretely obtain the value of the control vector, and apply the method to the systems. Finally, we illustrate circuit laboratory experiments and confirm the validity of the method.

2 | SYSTEM DESCRIPTION

Let us consider an n-dimensional switched dynamical system composed of two autonomous dynamical systems as follows:

$$\begin{aligned} \text{system } \alpha \ : \ \frac{d\boldsymbol{x}}{dt} &= \boldsymbol{f}_\alpha(\boldsymbol{x}, \lambda, \lambda_\alpha), \\ \text{system } \beta \ : \ \frac{d\boldsymbol{x}}{dt} &= \boldsymbol{f}_\beta(\boldsymbol{x}, \lambda, \lambda_\beta), \end{aligned} \tag{1}$$

where $t \in \boldsymbol{R}$ is the time, $\boldsymbol{x} \in \boldsymbol{R}^n$ is a state vector, and $\lambda \in \boldsymbol{R}^r$ is the vector containing the parameters shared by $\boldsymbol{f}_\alpha$ and $\boldsymbol{f}_\beta$. The parameter vectors λ_α and $\lambda_\beta \in \boldsymbol{R}^s$ are the vectors containing the parameters depending on $\boldsymbol{f}_\alpha$ and $\boldsymbol{f}_\beta$, respectively. Assume that $\boldsymbol{f}_\alpha$ and $\boldsymbol{f}_\beta$ are C^∞ functions with respect to any states and parameters. The solutions to $\boldsymbol{f}_\alpha$ and $\boldsymbol{f}_\beta$ together with an initial condition $\boldsymbol{x}_0$ are given as follows:

$$\begin{aligned} \text{system } \alpha \ : \ \boldsymbol{x}(t) &= \boldsymbol{\varphi}_\alpha(t, \boldsymbol{x}_0, \lambda, \lambda_\alpha), \\ \text{system } \beta \ : \ \boldsymbol{x}(t) &= \boldsymbol{\varphi}_\beta(t, \boldsymbol{x}_0, \lambda, \lambda_\beta). \end{aligned} \tag{2}$$

For implementation of a switching rule between the systems α and β, let us define a switching section Σ, which is the threshold switching the system from α to β:

$$\Sigma = \left\{ \boldsymbol{x} \in \boldsymbol{R}^n \quad | \quad q(t, \boldsymbol{x}, \lambda_r) = 0 \right\}, \tag{3}$$

where $q \ : \ \boldsymbol{R}^n \to \boldsymbol{R}$ is a scalar function determining the structure of the threshold. Assume that q is a periodic function with period T:

$$q(t + T, \boldsymbol{x}, \lambda_r) = q(t, \boldsymbol{x}, \lambda_r), \tag{4}$$

where λ_r is a parameter vector. Notice that any parameter in λ_r is not included in $\boldsymbol{f}_\alpha$ and $\boldsymbol{f}_\beta$. The rules for the switching of the systems are as follows:

1. the system is obeyed by the system α when the clock signal, which is externally applied with the period T,
2. the system changes from α to β when the state arrives at Σ.

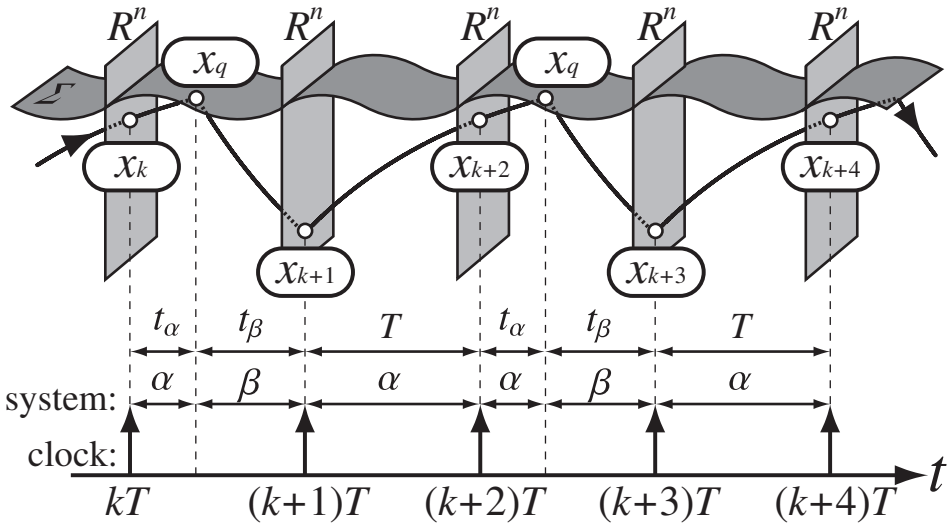

FIGURE 1 Schematic illustration of the solution to a n-dimensional switched dynamical system.

Figure 1 shows the example of the solution and switching with an initial condition $\boldsymbol{x}_k = \boldsymbol{x}(kT)$. In the figure, $\boldsymbol{x}_q$ is the state arriving at Σ, t_α is the interval from $\boldsymbol{x}_k$ to $\boldsymbol{x}_q$, and t_β is the interval from $\boldsymbol{x}_q$ to $\boldsymbol{x}_{k+1}$.

When a solution to the system (1) satisfies

$$\boldsymbol{x}(t+T) = \boldsymbol{x}(t), \tag{5}$$

the solution is called *a periodic orbit*. Similarly, when a solution satisfies

$$\boldsymbol{x}(t+mT) = \boldsymbol{x}(t), \tag{6}$$

the solution is called *an m-periodic orbit*. Let $\boldsymbol{M}$ be the Poincaré map of the periodic solution of the system (1) together with $\boldsymbol{x}_k$ as

$$\boldsymbol{M} : \boldsymbol{R}^n \to \boldsymbol{R}^n; \quad \boldsymbol{x}_k \mapsto \boldsymbol{x}_{k+1}. \tag{7}$$

The state $\boldsymbol{x}^*$ is called *an m-periodic point* of $\boldsymbol{M}$ if $\boldsymbol{x}^* = \boldsymbol{M}^m(\boldsymbol{x}^*)$. m-periodic points are on a periodic orbit or an m-periodic orbit. A 1-periodic point is also called *a fixed point*.

3 | THE METHOD TO STABILIZE UNSTABLE PERIODIC ORBITS

In this section, we propose a method to stabilize an unstable m-periodic orbit which is based on the method of Ito[23]. We choose a control parameter $\lambda_d \in \lambda_r$, which is the parameter of the function q.

Our method is based on the variational equation of the system along its unstable m-periodic orbit. To derive the variational equation, we introduce the local map from $\boldsymbol{x}_k$ to $\boldsymbol{x}_{k+1}$, and its derivative with respect to the initial conditions and the control parameter.

In the case of $t_\alpha \geq T$, that is, the solution together with $\boldsymbol{x}_k$ does not arrive at Σ within the period T, the Poincaré map from $\boldsymbol{x}_k$ to $\boldsymbol{x}_{k+1}$ is given by

$$\boldsymbol{M}_k^{[1]} : \boldsymbol{R}^n \to \boldsymbol{R}^n; \quad \boldsymbol{x}_k \mapsto \boldsymbol{x}_{k+1} = \boldsymbol{\varphi}_\alpha(T, \boldsymbol{x}_k, \lambda, \lambda_\alpha). \tag{8}$$

With defining the variation $\boldsymbol{\xi}$ along an m-periodic point $\boldsymbol{x}^*$ and the control input u for λ_d:

$$\boldsymbol{x}(k) = \boldsymbol{x}^* + \boldsymbol{\xi}(k), \quad \lambda_d(k) = \lambda_d^* + \boldsymbol{u}(k), \tag{9}$$

the variational equation of $\boldsymbol{M}^{[1]}$ along $\boldsymbol{x}^*$ is written by

$$\boldsymbol{\xi}(k+1) = \boldsymbol{A}_k^{[1]}\boldsymbol{\xi}(k) + \boldsymbol{B}_k^{[1]}u(k), \tag{10}$$

where

$$\boldsymbol{A}_k^{[1]} = \frac{\partial \boldsymbol{M}_k^{[1]}}{\partial \boldsymbol{x}_k}, \quad \boldsymbol{B}_k^{[1]} = \frac{\partial \boldsymbol{M}_k^{[1]}}{\partial \lambda_d} = \boldsymbol{0}. \tag{11}$$

The variation of λ_d cannot affect the value of $M_k^{[1]}$ because the solution does not arrive at Σ. Therefore, the second equation of Eq. (11) becomes $\mathbf{0}$.

In the case of $t_\alpha < T$, that is, in the case that the solution together with $\boldsymbol{x}_k$ arrives at Σ within the period T, the Poincaré map from $\boldsymbol{x}_k$ to $\boldsymbol{x}_{k+1}$ is given by the composition of local maps M_α and M_β as follows:

$$\begin{aligned} M_\alpha &: \boldsymbol{R}^n \to \Sigma; \\ &\quad \boldsymbol{x}_k \mapsto \boldsymbol{x}_q = \boldsymbol{\varphi}_\alpha(t_\alpha(\boldsymbol{x}_k, \lambda_d), \boldsymbol{x}_k, \lambda, \lambda_\alpha), \\ M_\beta &: \Sigma \to \boldsymbol{R}^n; \\ &\quad \boldsymbol{x}_q \mapsto \boldsymbol{x}_{k+1} = \boldsymbol{\varphi}_\beta(T - t_\alpha(\boldsymbol{x}_k, \lambda_d), \boldsymbol{x}_q, \lambda, \lambda_\beta), \\ M_k^{[2]} &: \boldsymbol{R}^n \to \boldsymbol{R}^n; \\ &\quad \boldsymbol{x}_k \mapsto \boldsymbol{x}_{k+1} = M_\beta \circ M_\alpha. \end{aligned} \tag{12}$$

At this time, the variational equation of $M^{[2]}$ along $\boldsymbol{x}^*$ is written by

$$\boldsymbol{\xi}(k+1) = \boldsymbol{A}_k^{[2]} \boldsymbol{\xi}(k) + \boldsymbol{B}_k^{[2]} u(k), \tag{13}$$

where

$$\begin{aligned} \boldsymbol{A}_k^{[2]} &= \frac{\partial M_k^{[2]}}{\partial \boldsymbol{x}_k} = \frac{\partial M_\beta}{\partial \boldsymbol{x}_q} \frac{\partial M_\alpha}{\partial \boldsymbol{x}_k} + \frac{\partial M_\beta}{\partial \boldsymbol{x}_k} \\ &= \frac{\partial \boldsymbol{\varphi}_\beta}{\partial \boldsymbol{x}_q} \left(\frac{\partial \boldsymbol{\varphi}_\alpha}{\partial \boldsymbol{x}_k} + \left. \frac{\partial \boldsymbol{\varphi}_\alpha}{\partial t} \right|_{t=t_\alpha} \frac{\partial t_\alpha}{\partial \boldsymbol{x}_k} \right) + \left. \frac{\partial \boldsymbol{\varphi}_\beta}{\partial t} \right|_{t=T-t_\alpha} \left(-\frac{\partial t_\alpha}{\partial \boldsymbol{x}_k} \right), \end{aligned} \tag{14}$$

$$\begin{aligned} \boldsymbol{B}_k^{[2]} &= \frac{\partial M_k^{[2]}}{\partial \lambda_d} = \frac{\partial M_\beta}{\partial \boldsymbol{x}_q} \frac{\partial M_\alpha}{\partial \lambda_d} + \frac{\partial M_\beta}{\partial \lambda_d} \\ &= \frac{\partial \boldsymbol{\varphi}_\beta}{\partial \boldsymbol{x}_q} \left(\left. \frac{\partial \boldsymbol{\varphi}_\alpha}{\partial t} \right|_{t=t_\alpha} \frac{\partial t_\alpha}{\partial \lambda_d} \right) + \left. \frac{\partial \boldsymbol{\varphi}_\beta}{\partial t} \right|_{t=T-t_\alpha} \left(-\frac{\partial t_\alpha}{\partial \lambda_d} \right). \end{aligned} \tag{15}$$

The derivatives of t_α with respect to $\boldsymbol{x}_k$ and λ_d are derived from the derivatives of the function q with respect to $\boldsymbol{x}_k$ and λ_d. Finally, the derivatives of t_α are given as follows:

$$\begin{aligned} \frac{\partial t_\alpha}{\partial \boldsymbol{x}_k} &= -\frac{\dfrac{\partial q}{\partial \boldsymbol{x}} \dfrac{\partial \boldsymbol{\varphi}_\alpha}{\partial \boldsymbol{x}_k}}{\dfrac{\partial q}{\partial \boldsymbol{x}} \left. \dfrac{\partial \boldsymbol{\varphi}_\alpha}{\partial t} \right|_{t=t_\alpha} + \left. \dfrac{\partial q}{\partial t} \right|_{t=t_\alpha}}, \\ \frac{\partial t_\alpha}{\partial \lambda_d} &= -\frac{\dfrac{\partial q}{\partial \lambda_d}}{\dfrac{\partial q}{\partial \boldsymbol{x}} \left. \dfrac{\partial \boldsymbol{\varphi}_\alpha}{\partial t} \right|_{t=t_\alpha} + \left. \dfrac{\partial q}{\partial t} \right|_{t=t_\alpha}}. \end{aligned} \tag{16}$$

$\partial q / \partial t|_{t=t_\alpha} = 0$ if the function q is a constant value; and then, the variational equation (13) is exactly the same as the corresponding equation in Ref.[23]. Hence, our method is applicable to both systems: the system with a periodically moving threshold and the system with a constant threshold.

By combining Eq. (10) and Eq. (13), the composed Poincaré map M^m of an m-periodic orbit is given by

$$\begin{aligned} M^m &: \boldsymbol{R}^n \to \boldsymbol{R}^n; \\ &\quad \boldsymbol{x}_k \mapsto \boldsymbol{x}_{k+1} = M_{k+m-1}^{[l]} \circ \cdots M_{k+1}^{[l]} \circ M_k^{[l]}, \end{aligned} \tag{17}$$

where $l \in \{1, 2\}$. The variational equation along the corresponding m-periodic point is

$$\boldsymbol{\xi}(k+m) = \boldsymbol{A} \boldsymbol{\xi}(k) + \boldsymbol{B} \boldsymbol{u}(k), \tag{18}$$

where

$$\boldsymbol{A} = \boldsymbol{A}_{k+m-1}^{[l]} \cdots \boldsymbol{A}_{k+1}^{[l]} \boldsymbol{A}_k^{[l]} = \frac{\partial M}{\partial \boldsymbol{x}_k} = \prod_{p=1}^{m} \frac{\partial M_{k+m-p}^{[l]}}{\partial \boldsymbol{x}_{k+m-p}}, \tag{19}$$

$$\boldsymbol{B} = \boldsymbol{B}_{k+m-1}^{[l]} \cdots \boldsymbol{B}_{k+1}^{[l]} \boldsymbol{B}_k^{[l]} = \frac{\partial M}{\partial \boldsymbol{x}_k}. \tag{20}$$

Generally, we can obtain the matrices A and B by using the numerical integration such that Runge-Kutta method.

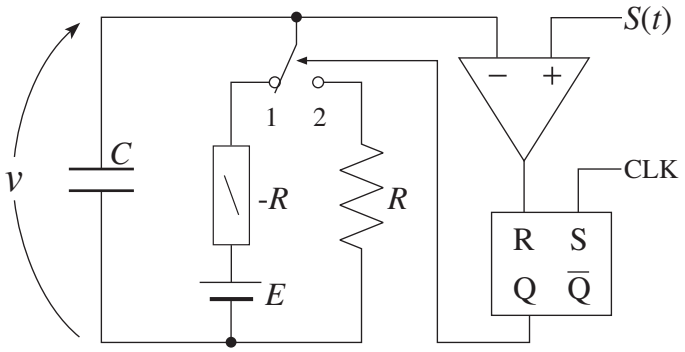

FIGURE 2 The circuit constructed of two linear dynamical systems.

If $m = 1$,

$$\frac{\partial M}{\partial \boldsymbol{x}_k} = \frac{\partial M_k^{[2]}}{\partial \boldsymbol{x}_k}, \tag{21}$$

and otherwise,

$$\frac{\partial M}{\partial \boldsymbol{x}_k} = \sum_{j=0}^{m-2} \left\{ \left(\prod_{p=1}^{m-(j+1)} \frac{\partial M_{k+m-p}^{[l]}}{\partial \boldsymbol{x}_{k+m-p}} \right) \frac{\partial M_{k+j}^{[l]}}{\partial \lambda_d} \right\} + \frac{\partial M_{k+m-1}^{[l]}}{\partial \lambda_d}. \tag{22}$$

The control input $\boldsymbol{u}(k)$ is given by

$$\boldsymbol{u}(k) = \boldsymbol{C}^\top \boldsymbol{\xi}(k) = \boldsymbol{C}^\top (\boldsymbol{x}_k - \boldsymbol{x}^*), \tag{23}$$

where $\boldsymbol{C}$ is a control vector.

The characteristic equation of the variational equation (18) is given with substituting Eq. (23) for Eq. (18) by

$$\det \left(\boldsymbol{A} + \boldsymbol{B}\boldsymbol{C}^\top - \mu I_n \right) = 0, \tag{24}$$

where I_n is an identity matrix with the size of $n \times n$.

The local stability along an m-periodic point of the system is controllable with applying an arbitrary linear control method, e.g., pole placement control, to Eq. (24). The control input is applied to λ_d if the following inequality is satisfied:

$$||\boldsymbol{x}_k - \boldsymbol{x}^*|| < \epsilon, \tag{25}$$

where $|| \cdot ||$ means Euclidean norm and ϵ is an arbitrary positive and small value.

4 | NUMERICAL EXPERIMENTS OF THE CONTROLLING METHOD

In this section, we numerically demonstrate the controlling method proposed in Sec. 3. For the simplicity, we treat a simple switched dynamical system composed of two linear dynamical systems, as shown in Fig. 2 . The circuit equation is given as follows:

$$RC\frac{dv}{dt} = \begin{cases} v - E & \text{if switch is toward 1,} \\ -v & \text{if switch is toward 2.} \end{cases} \tag{26}$$

Let us describe the system whose switch is toward 1 is the system 1, and the system whose switch is toward 2 is the system 2. In this circuit, $S(t)$ is a periodic function with period T, which corresponds the threshold q, and CLK is a clock pulse applied with the period T. The switching rule of this circuit is completely the same as the rule mentioned in Sec. 3. With rewriting $t/RC \to t$, the normalized equation of Eq. (26) is

$$\frac{dv}{dt} = \begin{cases} v - E & \text{if system 1,} \\ -v & \text{if system 2.} \end{cases} \tag{27}$$

Note that the period T of the function $S(t)$ should be replaced by RCT. The solutions to the system 1 and 2 are analytically solved as follows:

$$\begin{aligned} &\text{system 1} \ : \ v(t) = (v_k - E)e^{t-kT} + E, \\ &\text{system 2} \ : \ v(t) = v_k e^{-t+kT}, \end{aligned} \tag{28}$$

where $v_k = v(kT) \in \boldsymbol{R}$ and e is the base of the natural logarithm. From Eq. (28), v_k and v_{k+1} satisfy the following equation:

$$v_{k+1} = \begin{cases} (v_k - E)e^T + E & \text{if } t_1(v_k) \geq T, \\ (v_k - E)e^{-T+2t_1(v_k)} + Ee^{-T+t_1(v_k)} & \text{if } t_1(v_k) < T, \end{cases} \tag{29}$$

where $t_1(v_k)$ is the time when the solution departing from v_k arrives the threshold.

The following steps are the procedure to construct the controlling system for numerical experiments.

Step. 1 Preliminary clarify the position of the m-periodic point v^* existing in chaos. For example, if v^* is the fixed point, this is obtained by solving $v_{k+1} = v_k = v^*$. Consequently, from Eq. (29), the solution to the following equation equals to the position of the fixed point v^*:

$$v^* - (v^* - E)e^{-T+2t_1(v^*)} + Ee^{-T+t_1(v^*)} = 0. \tag{30}$$

We numerically solve Eq. (30) by Newton's method.

Step. 2 Calculate $\boldsymbol{A}$ and $\boldsymbol{B}$ in Eq. (18) for v^*.

Step. 3 Derive the control vector $\boldsymbol{C}$. Generally, $\boldsymbol{B}$ is a matrix if Eq. (24) is satisfied; and then, $\boldsymbol{C}$ is derived from Eq. (24). We call this $\boldsymbol{C}$ *a control gain*. For simplicity, we assume a dead-beat control, i.e., we choose $\mu = 0$ here.

Step. 4 Determine the control boundary. The control input (23) is applied to the control parameter if the following condition is satisfied:

$$|v_k - v^*| < \epsilon, \tag{31}$$

where, in this instance, we set $\epsilon = 0.3$.

Let us apply these steps to the following practical examples.

4.1 | A sine wave threshold

The scheme of sinusoidal pulse width modulation[25] includes the sinusoidal reference voltage. Similarly, we consider a case that the function $S(t)$ is a sine wave:

$$S(t) = V \sin \Omega t + V_0, \quad \Omega = \frac{2\pi}{T}, \tag{32}$$

where V, V_0 and Ω are the amplitude, the DC component, and the angular velocity, respectively. At this time, $t_1(v_k)$ in Eq. (29) is numerically calculated by solving the following equation with Newton's method:

$$(v_k - E)e^{t_1(v_k)} + E - V \sin \Omega t_1(v_k) - V_0 = 0. \tag{33}$$

We choose the constant values for the following parameters:

$$\begin{aligned} &R = 10\ [\mathrm{k}\Omega], \quad C = 0.1\ [\mu\mathrm{F}], \quad E = 1.4\ [\mathrm{V}], \\ &T = 0.5\ [\mathrm{ms}], \quad V = 0.1\ [\mathrm{V}], \quad V_0 = 0.3\ [\mathrm{V}]. \end{aligned} \tag{34}$$

Let us stabilize unstable periodic orbits to control the chaos of the system (27) whose threshold is the sine wave. We assume that the control parameter is V_0; then the control input $u(k)$ is applied to $S(t)$. Figure 3 shows the chaos that we control. As Step. 2, for the fixed point v_1^*, we need not to use the numerical integration for obtaining $\boldsymbol{A}$ and $\boldsymbol{B}$ since the system is piecewise linear. In this case, $\boldsymbol{A}$ and $\boldsymbol{B}$ are analytically given by differentiating Eq. (29) with respect to v_k:

$$\begin{aligned} \boldsymbol{A} &= \frac{dv_{k+1}}{dv_k} = Ee^{-T+t_1(v_k)}\frac{\partial t_1(v_k)}{\partial v_k} + e^{-T+2t_1(v_k)} + 2(v_k - E)e^{-T+2t_1(v_k)}\frac{\partial t_1(v_k)}{\partial v_k}, \\ \boldsymbol{B} &= \frac{dv_{k+1}}{dV_0} = 2(v_k - E)e^{-T+2t_1(v_k)}\frac{\partial t_1(v_k)}{\partial V_0} + Ee^{-T+t_1(v_k)}\frac{\partial t_1(v_k)}{\partial V_0}. \end{aligned} \tag{35}$$

Partial derivatives of $t_1(v_k)$ with respect to v_k and V_0 are derived by differentiating Eq. (33) as follows:

$$\begin{aligned} \frac{\partial t_1(v_k)}{\partial v_k} &= -\frac{e^{t_1(v_k)}}{(v_k - E)e^{t_1(v_k)} - V\Omega \cos \Omega t_1(v_k)}, \\ \frac{\partial t_1(v_k)}{\partial V_0} &= \frac{1}{(v_k - E)e^{t_1(v_k)} - V\Omega \cos \Omega t_1(v_k)}. \end{aligned} \tag{36}$$

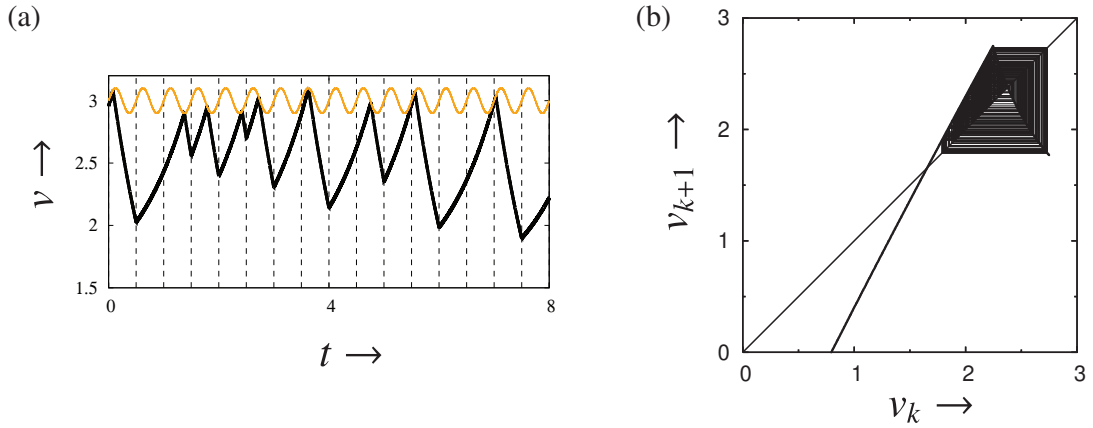

FIGURE 3 (a) Time waveform of the chaos in the system (27) with a sine wave, and (b) trajectory of the chaos in v_k-v_{k+1} plane.

TABLE 1 Position of m-periodic points in the system (27) with the sine wave, their characteristic multipliers, and the control gains, with $m = 1, 2$.

m	Position	Characteristic multiplier	Control gain $\boldsymbol{C}$
1	2.476491	−1.361377	0.747476
2	2.242971	−1.262122	0.923931

For the 2-periodic point v_2^*, $\boldsymbol{A}$ and $\boldsymbol{B}$ are also analytically given by

$$\begin{aligned} \boldsymbol{A} &= \frac{dv_{k+2}}{dv_k} = \frac{dv_{k+2}}{dv_{k+1}}\frac{dv_{k+1}}{dv_k}, \\ \boldsymbol{B} &= \frac{dv_{k+2}}{dV_0} = \frac{dv_{k+2}}{dv_{k+1}}\frac{dv_{k+1}}{dV_0} + \frac{dv_{k+2}}{dV_0}. \end{aligned} \tag{37}$$

The derivatives in Eq. (37) are computed by follows:

$$\begin{aligned} \frac{dv_{k+2}}{dv_{k+1}} &= e^{-T+2t_1(v_{k+1})}\left\{1 - \frac{2(v_{k+1}-E)e^{t_1(v_{k+1})}+E}{(v_{k+1}-E)e^{t_1(v_{k+1})} - V\Omega\cos\Omega t_1(v_{k+1})}\right\}, \\ \frac{dv_{k+1}}{dv_k} &= e^T, \\ \frac{dv_{k+2}}{dV_0} &= e^{-T+t_1(v_{k+1})}\left\{\frac{2(v_{k+1}-E)e^{t_1(v_{k+1})}+E}{(v_{k+1}-E)e^{t_1(v_{k+1})} - V\Omega\cos\Omega t_1(v_{k+1})}\right\}, \\ \frac{dv_{k+1}}{dV_0} &= 0, \end{aligned} \tag{38}$$

where the partial derivatives of $t_1(v_k)$ are replaced as Eq. (36). Table 1 shows the position of m-periodic points, their characteristic multipliers, and the control gain computed by Step. 1 to Step. 3.

Figure 4 shows the results of controlling. Before starting a control, in the shaded regions in each figure, the system (27) yields chaos as shown in Fig. 3 . Then, if the condition (31) is satisfied, the control input $u(k)$ of Eq. (23) is applied to $S(t)$. After that, each orbit rapidly approaches to each target solution. In other words, the chaos in each figure is stabilized to the periodic solution. In addition, after starting a control, we find the control input $u(k)$ converges to 0 as time grows. This results in that the proposed method is enough ideal to control chaos.

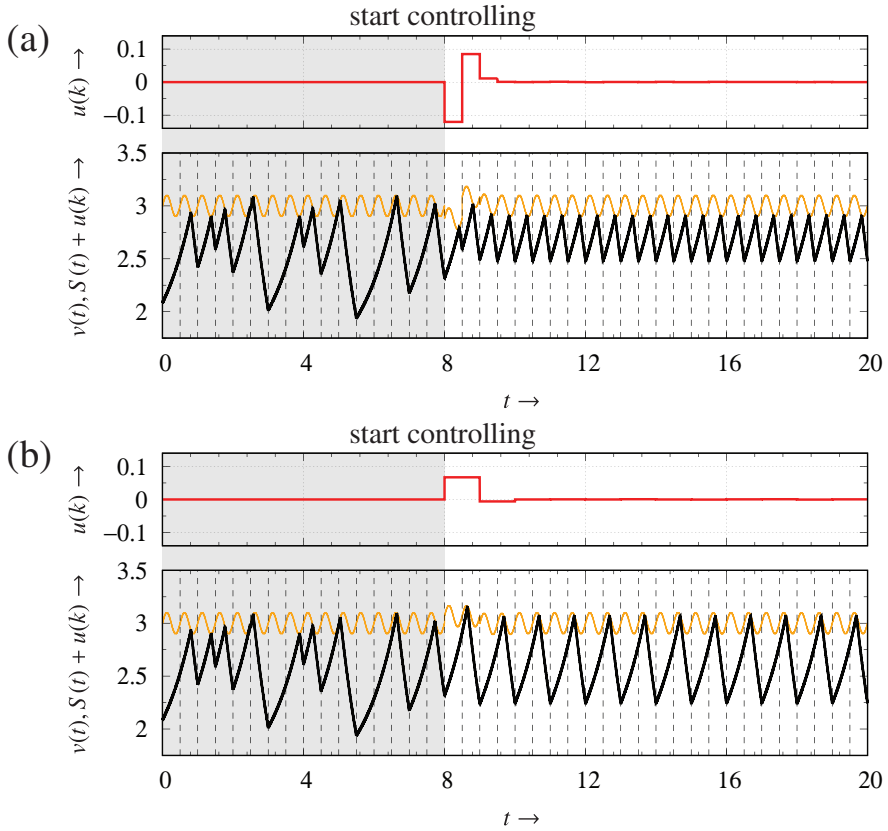

FIGURE 4 Time waveforms of the system (27) with a sine wave before and after starting a control. (a) Time waveform controlled to the 1-periodic orbit. (b) Time waveform controlled to the 2-periodic orbit.

4.2 | A sawtooth wave threshold

A sawtooth wave is well used as the reference voltage in the pulse width modulation[27]. We consider a case that the function $S(t)$ is a sawtooth wave:

$$S(t) = v_r - \frac{h}{T}(t \bmod T), \tag{39}$$

where v_r, h are the DC component and the amplitude of the sawtooth wave, respectively, and $(\cdot \bmod \cdot)$ is the modulo operation of the real numbers, e.g., $(0.27 \bmod 0.2) = 0.07$. At this time, $t_1(v_k)$ is numerically calculated by solving the following equation with Newton's method:

$$(v_k - E)e^{t_1(v_k)} + E - v_r + \frac{h}{T}(t_1(v_k) \bmod T) = 0. \tag{40}$$

We choose the constant values for the following parameters:

$$\begin{aligned} R &= 10\ [\mathrm{k}\Omega], \quad C = 0.33\ [\mu\mathrm{F}], \quad E = 1.4\ [\mathrm{V}], \\ T &= 0.485\ [\mathrm{ms}], \quad v_r = 2.9\ [\mathrm{V}], \quad h = 0.2\ [\mathrm{V}]. \end{aligned} \tag{41}$$

Similarly to the case of the sine wave, let us control the chaos the system (27) whose threshold is the sawtooth wave with stabilizing an unstable fixed point v_1^* and an unstable 2-periodic point v_2^*. We assume that the control parameter is v_r; then the control input $u(k)$ is applied to $S(t)$. Figure 5 shows the chaos that we control.

In a case of the sawtooth wave, for the fixed point v_1^*, $\boldsymbol{A}$ is the same as Eq. (35) and $\boldsymbol{B}$ is analytically given by

$$B = \frac{dv_{k+1}}{dv_r} = 2(v_k - E)e^{-T+2t_1(v_k)}\frac{\partial t_1(v_k)}{\partial v_r} + Ee^{-T+t_1(v_k)}\frac{\partial t_1(v_k)}{\partial v_r}. \tag{42}$$

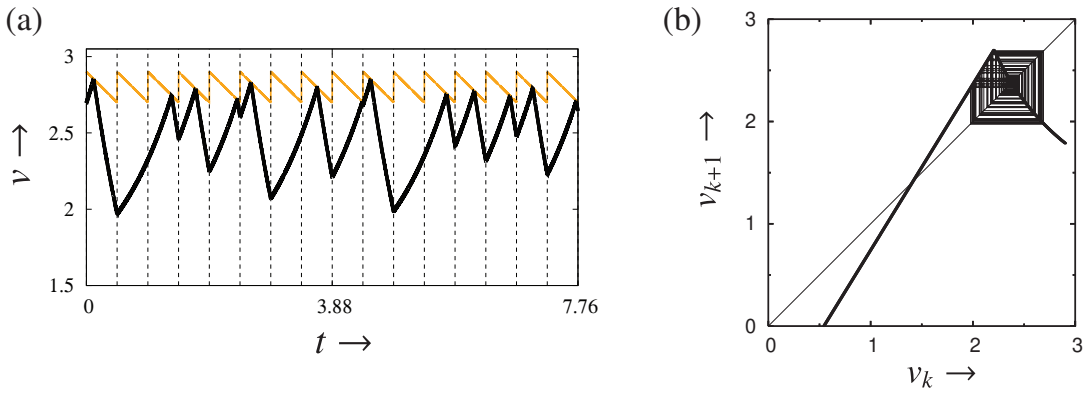

FIGURE 5 (a) Time waveform of the chaos in the system (27) with a sawtooth wave, and (b) trajectory of the chaos in v_k-v_{k+1} plane.

TABLE 2 Position of m-periodic points in the system (27) with the sawtooth wave, their characteristic multipliers, and the control gains, with $m = 1, 2$.

m	Position	Characteristic multiplier	Control gain $\boldsymbol{C}$
1	2.375331	−1.590389	0.795742
2	2.116001	−1.954534	1.124820

Partial derivatives of $t_1(v_k)$ with respect to v_k and v_r are derived by differentiating Eq. (40) as follows:

$$\begin{aligned}\frac{\partial t_1(v_k)}{\partial v_k} &= -\frac{e^{t_1(v_k)}}{(v_k - E)e^{t_1(v_k)} + \frac{h}{T}},\\ \frac{\partial t_1(v_k)}{\partial v_r} &= \frac{1}{(v_k - E)e^{t_1(v_k)} + \frac{h}{T}}.\end{aligned} \tag{43}$$

For the 2-periodic point v_2^*, $\boldsymbol{A}$ is the same as Eq. (37) and $\boldsymbol{B}$ are analytically given by

$$\boldsymbol{B} = \frac{dv_{k+2}}{dv_r} = \frac{dv_{k+2}}{dv_{k+1}}\frac{dv_{k+1}}{dv_r} + \frac{dv_{k+2}}{dv_r}. \tag{44}$$

The derivatives for $\boldsymbol{A}$ and $\boldsymbol{B}$ are computed by follows:

$$\begin{aligned}\frac{dv_{k+2}}{dv_{k+1}} &= e^{-T+2t_1(v_{k+1})}\left\{1 - \frac{2(v_{k+1} - E)e^{t_1(v_{k+1})} + E}{(v_{k+1} - E)e^{t_1(v_{k+1})} + \frac{h}{T}}\right\},\\ \frac{dv_{k+1}}{dv_k} &= e^T,\\ \frac{dv_{k+2}}{dv_r} &= e^{-T+t_1(v_{k+1})}\left\{\frac{2(v_{k+1} - E)e^{t_1(v_{k+1})} + E}{(v_{k+1} - E)e^{t_1(v_{k+1})} - \frac{h}{T}}\right\},\\ \frac{dv_{k+1}}{dv_r} &= 0,\end{aligned} \tag{45}$$

where the partial derivatives of $t_1(v_k)$ are replaced as Eq. (43). Table 2 shows the position of m-periodic points, their characteristic multipliers, and the control gain computed by Step. 1 to Step. 3.

Figure 6 shows the results of controlling. From the result, the controlling method also works reasonable.

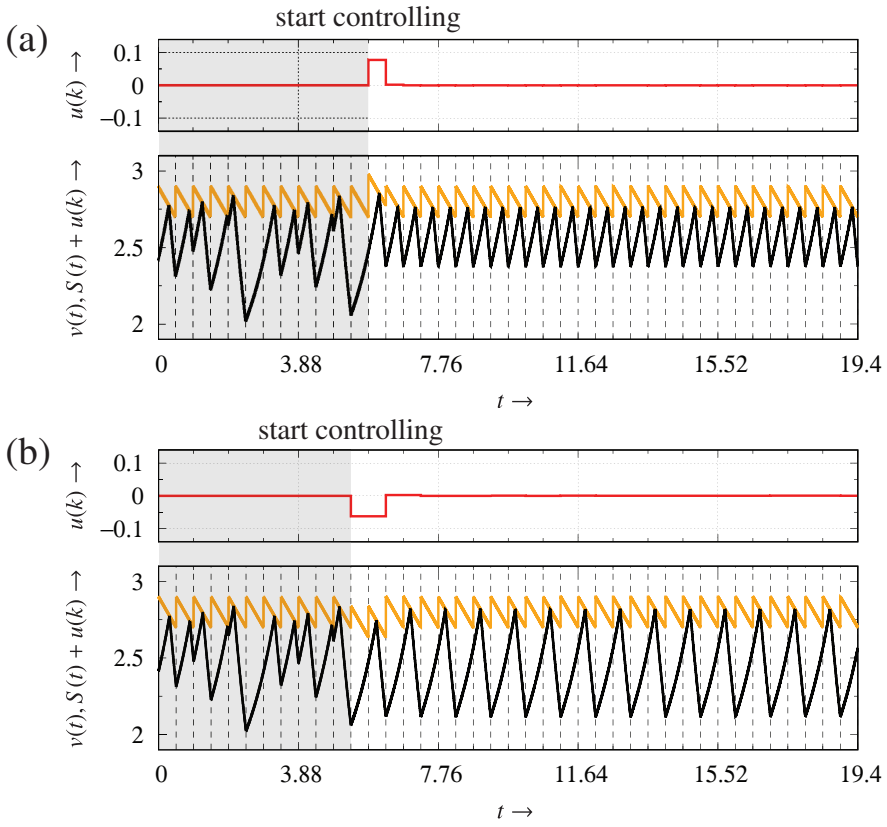

FIGURE 6 Time waveforms of the system (27) with a sawtooth wave before and after starting a control. (a) Time waveform controlled to the 1-periodic orbit. (b) Time waveform controlled to the 2-periodic orbit.

5 | CIRCUIT EXPERIMENTS OF THE CONTROLLING METHOD

In this section, we implement the proposed controlling method as a real circuit, shown in Fig. 7 . The controller is installed in the circuit in Fig. 2 , and is composed of a sample-hold circuit, a window comparator, a subtracting amplifier, an inverting amplifier, and a summing amplifier. A mechanism of the controller is described below.

1. The sample-hold circuit discretizes the voltage of capacitance with the period of the target unstable periodic orbit and applies the output voltage v_k to the subtracting amplifier and the window comparator.
2. The subtracting amplifier outputs the difference $\xi(k)$ between v_k and the voltage corresponding the target unstable periodic point.
3. The window comparator detects whether the voltage approaches the target or not. Consequently, if the inequality (31) is satisfied, the switch is turned into $1'$, and otherwise, the switch is turned into $2'$.
4. If the switch is toward $1'$, $\xi(k)$ is applied to the inverting amplifier. The inverting amplifier generates the control input $u(k)$ from $\xi(k)$ and $\boldsymbol{C}$, where we appropriately assign $\boldsymbol{C}$ from the ratio of R_2 to R_1 and applies it to the summing amplifier.
5. The summing amplifier outputs the voltage $v_{\text{out}} = u(k) + S(t)$.

5.1 | A sine wave threshold

In this part, we assume that $S(t)$ is the sine wave that we defined in Eq. (32). Let us fix the parameters as the same as Eq. (34). Figure 8 shows the result of the controlling. After starting the control, the time waveforms of Fig. 8 (a) and (b) rapidly converge to 1-periodic orbit and 2-periodic orbit, respectively. Their trajectory converge to 1 and 2 points in v_k-v_{k+1} plane, as shown in Fig. 8 (c) and (d).

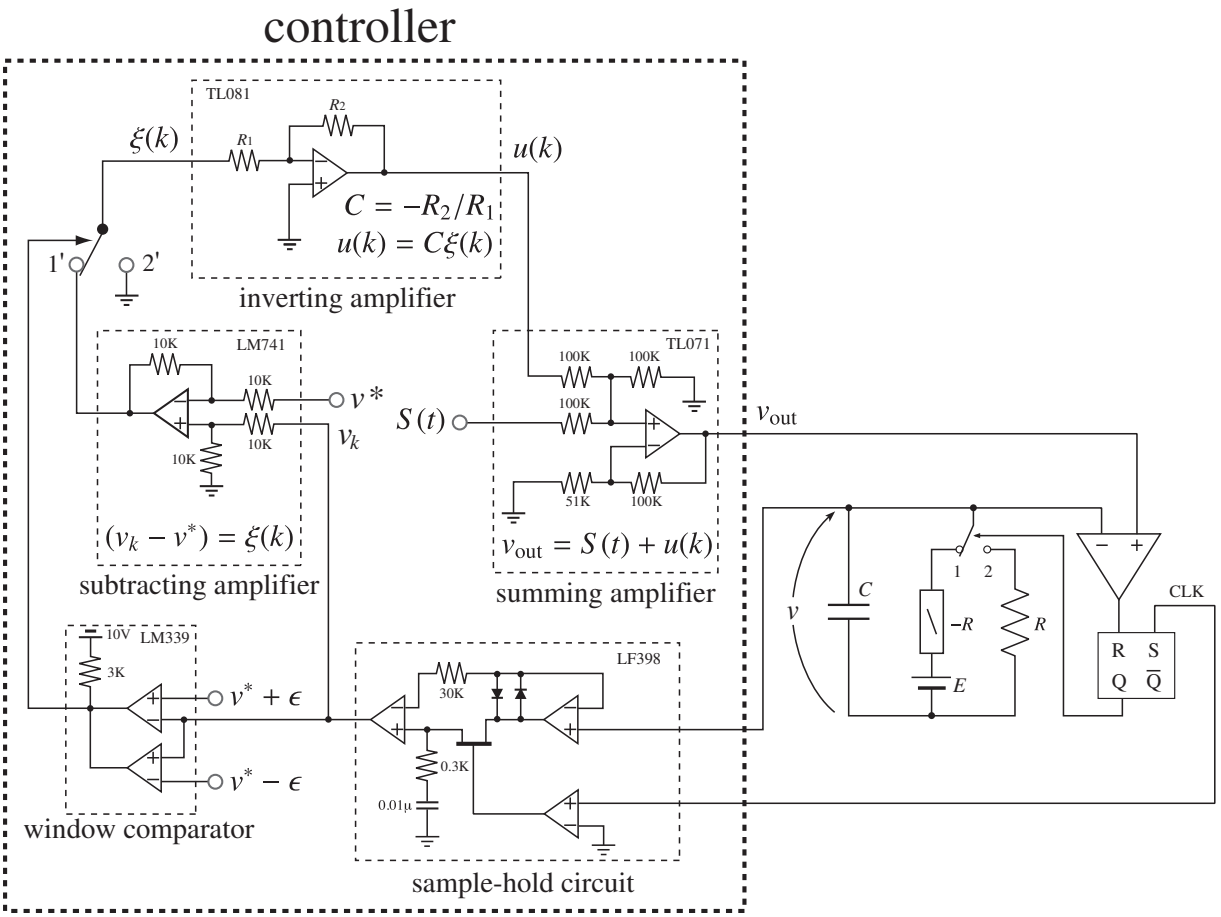

FIGURE 7 A controller implemented as a circuit.

5.2 | A sawtooth wave threshold

As another experiment , we assume that $S(t)$ is the sawtooth wave that we defined in Eq. (39). We also fix the parameters as the same as Eq. (41). Figure 9 shows the result of the controlling. Similarly to the previous section, the time waveforms of Fig. 9 (a) and (b) rapidly converge to 1-periodic orbit and 2-periodic orbit after starting the control, respectively. Their trajectories converge to show 1 and 2 points in v_k-v_{k+1} plane, as shown in Fig. 9 (c) and (d).

As the result, the proposed method has been valid for controlling the chaos in switched dynamical systems.

6 | CONCLUSION

In this study, we developed a generalized method to control the chaos in switched dynamical systems, which stabilizes an unstable periodic orbit by controlling the periodic threshold value. We first described an n-dimensional switched dynamical system, and introduced its behavior. For the mathematical construction of the controlling method, we defined two kinds of local maps and derived their derivatives with respect to the initial conditions and the control parameter. We finally implemented the proposed method in numerical simulations and confirmed validity of it. We also implemented the method in real circuits and found validity for it.

ACKNOWLEDGEMENT

This research is strongly supported by Yoshihiko Yamamoto who is a student in the laboratory of Takuji Kousaka.

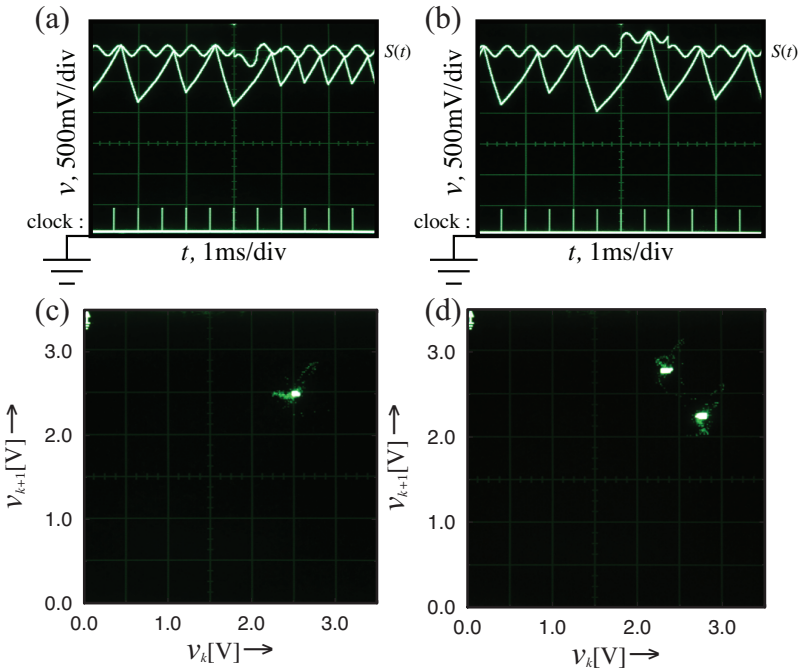

FIGURE 8 (a, b) Time waveforms of the circuit in Fig. 2 with the sine wave threshold and the controller in Fig. 7 , and (c, d) the trajectories of the circuit in v_k-v_{k+1} plane. (a) Controlling to a 1-periodic orbit, and (b) controlling to a 2-periodic orbit. The controlling starts from the center of each figure. (c) Trajectory corresponding the 1-periodic orbit in (a), and (d) trajectory corresponding the 2-periodic orbit in (b).

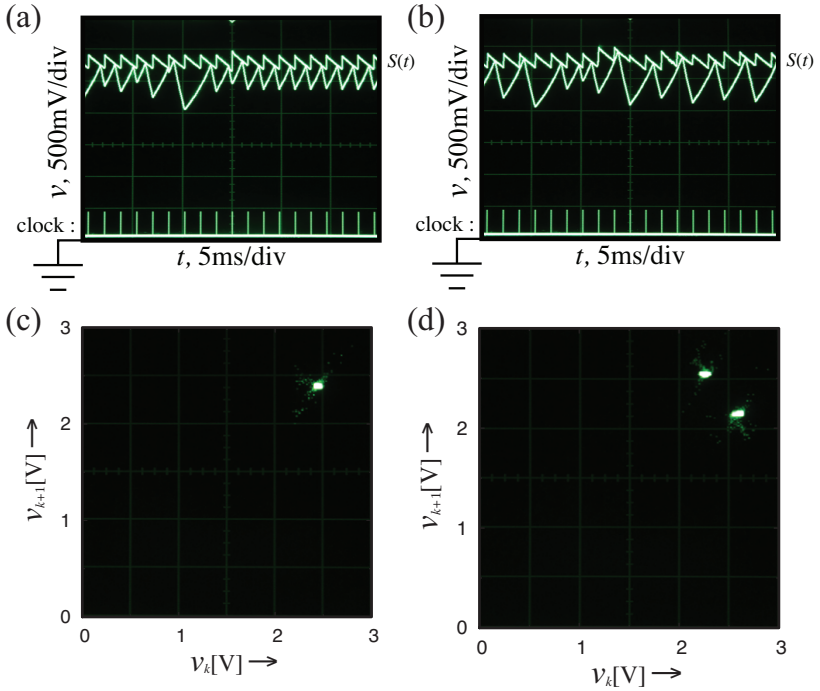

FIGURE 9 (a, b) Time waveforms of the circuit in Fig. 2 with the sawtooth wave threshold and the controller in Fig. 7 , and (c, d) the trajectories of the circuit in v_k-v_{k+1} plane. (a) Controlling to a 1-periodic orbit, and (b) controlling to a 2-periodic orbit. The controlling starts from the center of each figure. (c) Trajectory corresponding the 1-periodic orbit in (a), and (d) trajectory corresponding the 2-periodic orbit in (b).

References

1. Auerbach D, Cvitanović P, Eckmann J-P, Gunaratne G, Procaccia I. Exploring chaotic motion through periodic orbits. *Physical Review Letters.* 1987;58(23):2387.
2. Habutsu T, Nishio Y, Sasase I, Mori S. A secret key cryptosystem using a chaotic map. *IEICE Trans.*. 1990;E73(7):1041–1044.
3. Stojanovski T, Kocarev L. Chaos-based random number generators-part I: analysis [cryptography]. *IEEE Trans. on Circuits & Systs.*. 2001;48(3):281–288.
4. Aihara K, Takabe T, Toyoda M. Chaotic neural networks. *Physics letters A.* 1990;144(6-7):333–340.
5. Huang TL, Han XG, Lu JS. Chaos predication method based on Lyapunov exponent and its application in water quality forecast. *Journal of Xi'an University of Architecture & Technology (Natural Science Edition).* 2008;40(6):846–851.
6. Ott E, Grebogi C, Yorke JA. Controlling chaos. *Physical review letters.* 1990;64(11):1196.
7. Pyragas K. Continuous control of chaos by self-controlling feedback. *Physics letters A.* 1992;170(6):421–428.
8. Osipov G, Glatz L, Troger H. Suppressing chaos in the Duffing oscillator by impulsive actions. *Chaos, Solitons & Fractals.* 1998;9(1):307–321.
9. Lu Z, Shieh L-S, Chen G, Coleman NP. Simplex sliding mode control for nonlinear uncertain systems via chaos optimization. *Chaos, Solitons & Fractals.* 2005;23(3):747–755.
10. Yassen MT. Controlling chaos and synchronization for new chaotic system using linear feedback control. *Chaos, Solitons & Fractals.* 2005;26(3):913–920.
11. Rajasekar S, Lakshmanan M. Algorithms for controlling chaotic motion: application for the BVP oscillator. *Physica D: Nonlinear Phenomena.* 1993;67(1-3):282–300.
12. Myneni K, Barr TA, Corron NJ, Pethel SD. New method for the control of fast chaotic oscillations. *Physical Review Letters.* 1999;83(11):2175.
13. Zambrano S, Sanjuán MAF. Exploring partial control of chaotic systems. *Physical Review E.* 2009;79(2):026217.
14. Sabuco J, Zambrano S, Sanjuán MAF. Partial control of chaotic transients using escape times. *New Journal of Physics.* 2010;12(11):113038.
15. Miino Y, Ito D, Ueta T. A computation method for non-autonomous systems with discontinuous characteristics. *Chaos, Solitons & Fractals.* 2015;77:277–285.
16. Banerjee S. Coexisting attractors, chaotic saddles, and fractal basins in a power electronic circuit. *IEEE Trans. on Circuits & Systs.*. 1997;44(9):847–849.
17. Kousaka Takuji, Ueta Tetsushi, Kawakami Hiroshi. Bifurcation of switched nonlinear dynamical systems. *IEEE Trans. Circuits Systs.*. 1999;46(7):878–885.
18. Tse Chi Kong. *Complex behavior of switching power converters*. CRC press; 2003.
19. Banerjee Soumitro, Verghese George C. *Nonlinear phenomena in power electronics: Bifurcations, chaos, control, and applications*. Wiley-IEEE Press; 2001.
20. Kousaka T, Ueta T, Ma Y, Kawakami H. Control of chaos in a piecewise smooth nonlinear system. *Chaos, Solitons & Fractals.* 2006;27(4):1019–1025.
21. Natsheh AN, Kettleborough JG, Janson NB. Experimental study of controlling chaos in a DC–DC boost converter. *Chaos, Solitons & Fractals.* 2009;40(5):2500–2508.

22. Asahara H, Tasaki K, Aihara K, Kousaka T. The Stabilizing mechanism for an interrupted dynamical system with periodic threshold. *Nonlinear Theory and Its Applications, IEICE.* 2012;3(4):546–556.

23. Ito D, Ueta T, Kousaka T, Imura J, Aihara K. Controlling Chaos of Hybrid Systems by Variable Threshold Values. *Int. J. of Bifurcation and Chaos.* 2014;24(10):1450125.

24. Luck JM, Mehta A. Bouncing ball with a finite restitution: chattering, locking, and chaos. *Physical Review E.* 1993;48(5):3988.

25. Van DBHW, Skudelny H-C, Stanke GV. Analysis and realization of a pulsewidth modulator based on voltage space vectors. *IEEE Trans. on Industry Applications.* 1988;24(1):142–150.

26. Ueta T, Kawakami H. Composite dynamical system for controlling chaos. *IEICE Trans.*. 1995;E78-A(6):708–714.

27. Sun J. Pulse-width modulation. In: Springer 2012 (pp. 25–61).

AUTHOR BIOGRAPHY

Yuu Miino received the B.E. and M.E. degrees from Tokushima University, Tokushima, Japan, in 2014 and 2016, respectively. He is currently the Ph. D candidate in graduate school of advanced technology and science, Tokushima University. His research interest is bifurcation problem of nonlinear dynamical systems.

Daisuke Ito received the B.E., M.E. and D.E. degrees from Tokushima University, Tokushima, Japan, in 2010, 2012, and 2015, respectively. He is currently an Assistant Professor in Gifu University. His research interest is nonlinear phenomena and electronics.

Hiroyuki Asahara received the B.E., M.E. and D.E. degrees in the Department of Mechanical and Energy Systems Engineering in Oita University, Oita, Japan, in 2009 and 2011, respectively. He is currently a Lecturer in Okayama University of Science. He is a member of the IEEE. His research interest is nonlinear phenomena in the switched dynamical systems.

Takuji Kousaka received the Ph.D. degree in Tokushima University, Tokushima, Japan, in 1999. From 1999 to 2006 he was on the faculty of Fukuyama University, Fukuyama, Hiroshima, Japan. In 2006, he joined the Department of Mechanical and Energy Systems Engineering at Oita University, Oita, Japan, where he is currently an Associate Professor. His research interests include bifurcation analysis in a switched dynamical system and its application.

Tetsushi Ueta received the B.E., M.E. and D.E. degrees from Tokushima University, Tokushima, Japan, in 1990, 1992, and 1996, respectively. He is currently a professor of Center for Administration of Information Technology, Tokushima University. His research interests include bifurcation problems of nonlinear dynamical systems.